J. theor. Biol. (1995) **176,** 501–510

this paper specifically takes our chaos model as a basis and varies on the results by trying different functionals than the Holling type II response
they also do some theoretical analysis with stability maps - maybe this is applicable to our original paper
it gives a bit more explanation about bifurcation diagrams and the period doublings which are an argument for chaos

The Structural Stability of a Three-Species Food Chain Model

JOSEPH. N. EISENBERG† AND DON R. MASZLE‡

†*Division of Environmental Health Science, University of California at Berkeley and* ‡ *Joint Bioengineering Group, University of California at Berkeley/San Francisco*, 140 *Earl Warren Hall, School of Public Health, University of California at Berkeley, Berkeley, CA* 94720, *U.S.A.*

(*Received on* 22 *November* 1994, *Accepted in revised form on* 30 *May* 1995)

A three-species food-chain model which was previously shown to exhibit chaotic dynamics was revisited. By exploring the sensitivity of that result this study found that complex behavior depended on the functional form chosen to model the interaction between the two highest species in the food chain. Two separate scenarios were explored: the gradual addition of refugia modeling the escape from predation at low prey densities; and the gradual addition of predator interference modeling territorial behavior. The addition of even a small amount of refugia provided a stabilizing influence as the chaotic dynamics collapsed to stable limit cycles. The results of adding interference to the model were more complex. Although the numerical simulations indicated that a low level of interference provided a stabilizing influence, the analytical results suggest that complex dynamics are possible for a range of parameter values that are biologically relevant. The sensitivity of the stability profile to functional changes in the model suggests two important ecological motivations for structural stability analysis. First, in ecological systems, environmental fluctuations cause continuous changes in the functional relationships between and within species, resulting in potential changes in the complexity of the dynamics over time. Second, slight changes in ecological structure may cause significant bifurcations; however, most ecological data are inadequate to distinguish such phenomena.

Introduction

Ecological systems have all the elements to produce chaotic dynamics: for example high gains, high levels of nonlinearities and significant time delays. High gains are common for both plants and insects which can produce hundreds or even thousands of offspring. Nonlinearities often occur in the form of saturations when there are limitations on the consumption or uptake of resources. Significant time delays are often due to maturation of organisms or the flow of nutrients through ecosystems. One would thus expect chaotic dynamics to exist in these systems. Although Sugihara & May (1990) were successful in distinguishing between dynamical chaos and measurement errors in short-term (1 to 2 years) infectious disease data, no one has shown that these results can be generalized to address the chaotic nature of ecosystems. The difficulty is due to the uncertain nature of experimental data; consequently, much of the work in exploring chaos in natural ecosystems has been theoretical.

it's hard to be sure chaos is occuring or if data is just too noisy

Several ecological models show that complex dynamics can result from simulation using simple equations and relationships (May & Oster 1976; Gilpin & Mackey, 1979; Hastings & Powell, 1991; Logan & Hain, 1991; Abrams & Roth, 1994; Hastings & Higgins, 1994). However, to assess the ecological implications of these findings, it is important to explore changes in the dynamics when structural assumptions of the system are varied. In this context, the use of the term structure is a mathematical one, and should not be confused with its use in describing community or food web structure. All models have assumptions which can critically affect the implications or conclusions derived from them. Some assumptions relate to the uncertainty of parameter values while

E-mail: † eisenber@garnet.berkeley.edu and ‡ maze@lrf563.berkeley.edu.

others relate to the structure or functional form of the model. For parameter values, often only certain ranges of parameters produce a model that is validated by data. The behavior of a model can also be dependent on assumptions inherent in the functional forms chosen for the equations. In this case, the observed behavior could be the result of choosing one functional form over another for a particular process, rather than a general quality of the interactions being studied.

This paper extends the work of Hastings & Powell (1991) by exploring the sensitivity of their results to the phenomenological assumptions of consumption. In their study, Hastings and Powell showed that chaotic population dynamics were exhibited by a simple three-species food chain model in which species interactions were described by the Holling II function. For biologically relevant parameter values, the model produced chaos over a range of the half-saturation constant of the Holling function. Our study explores the structural stability of this three-species model by specifically focusing on the effects of two structural variations to the Holling II response; one increases the refugia of prey and the other increases the self-interference of consumers.

For low prey densities, the Holling II function describes consumption by predation as an increasing function of prey, until at higher prey densities the rate of consumption saturates because each predator can only handle a finite number of prey in a unit of time. To describe decreased predation at lower prey densities, such as when refugia are present, a Holling Type III function is traditionally used. This function was first introduced by Holling (1959) and has been explored further by many researchers (Real, 1977; Hassell, 1978; Nunney, 1980; DeAngelis, 1992). The use of the sigmoidal type III functional response is a good model for many invertebrate systems (Hassell & Comins, 1978). Many other behaviors that can be modeled using a Type III function have been described by Krebs (1974). These include predators switching to different prey (Murdoch, 1969), predators learning to handle prey better with increased experience (Orians, 1969), and predators learning to alter their search pattern to maximize prey encounters (Dixons, 1959).

To characterize interference between consumers, authors have modified the Type II functional response (DeAngelis *et al*., 1975; Getz, 1984), such that as the consumer density increases the consumption rate decreases. Experimental studies have produced data which suggest the existence of consumer interference responses in ecological systems (Arditi *et al*., 1991*a*, *b*; Akcakaya, 1992; Arditi & Saiah, 1992), while theoretical studies have compared stability characteristics of the consumer interference response with other response functions (Berryman, 1992).

Model Formulation

For comparative purposes, we have chosen to use the same three-species model as Hastings & Powell (1991) with one functional modification. Their model is shown here in non-dimensionalized form.

$$\frac{dx}{dt} = x(1-x) - f_1(x)y$$

$$\frac{dy}{dt} = f_1(x)y - f_2(y)z - d_1 y$$

$$\frac{dz}{dt} = f_2(y)z - d_2 z, \tag{1}$$

where x represents the number of individuals at the lowest level of the food chain, y the number of individuals that prey on x, and z the number of individuals that prey on y. The functions f_1 and f_2 represent the predation of y on x and z on y respectively, and d_1 and d_2 are constant death rates for species y and z, respectively.

Three typical removal rate functions used in food chain models are of interest in this study. They are the Holling II and Holling III (Holling, 1959) functions, given by

$$F^{(II)}(x) = \frac{ax}{1+bx} \tag{2}$$

$$F^{(III)}(x) = \frac{ax^2}{1+bx^2} \tag{3}$$

and a variant of the Holling Type II function characterizing consumer interference (DeAngelis *et al*., 1975; Getz, 1993) given by

$$F^{(C)}(x) = \frac{ax}{1+bx+\gamma y}. \tag{4}$$

All of these functions describe a saturation effect whereby as the prey density increases, the predation rate becomes less dependent on the population of the prey and only dependent on the predator population. Additionally, the Holling III function describes a decreased rate of predation at low prey densities, while the consumer interference function describes a decreased rate of predation at high predator densities.

In this study we used the function $F^{(II)}$ [eqn (2)] to describe the x–y interaction, and the following function to describe the y–z interaction;

$$f_2(y, \epsilon) = \frac{a_2 y^{\epsilon}}{1+b_2 y^{\epsilon}+\gamma z}, \tag{5}$$

where with $\gamma = 0, \epsilon = 1$ describes the Holling II and $\epsilon = 2$ describes the Holling III functional responses. Values of ϵ between 1 and 2 describe imperfect refugia where at low densities prey may be harder to find compared with at high densities. The interference parameter γ describes the effects of interference by making the functional response dependent on the consumer interference availability of prey to the predators. Therefore, f_2 is a function which incorporates the characteristics of functions (2), (3) and (4).

We devised two scenarios to explore the sensitivity of chaotic dynamics to the independent variation of two factors, refugia and interference, which affect predation. In scenario 1, ϵ ranged from 1 to 2 with γ set to zero, and in scenario 2 γ ranged from 0 to 2 with ϵ set to 1. The x–y interaction was not modified since a density dependency already was included in the x mortality term, producing a similar stabilizing effect as would the addition of a Holling Type III interaction.

Analysis

Both analytical and numerical simulations were performed. Analytical studies were used as an initial means to look at stability conditions in the parameter space of the model. In the first scenario where we modeled refugia, the equilibrium points, $\bar{\mathbf{x}}$, of the state vector $\mathbf{x} = \{x, y, z\}$ were solved as a function of all parameters and then interpreted for the parameter set that Hastings and Powell investigated with the addition of the exponent parameter, ϵ, and γ set to zero. Their choice of parameters was based on an interest in eliciting chaotic dynamics and consisted of the following two constraints: that the x–y interactions occur on a faster timescale than the y–z dynamics, and that the x–y dynamics were oscillatory in the absence of z. Table 1 lists the parameter values for the model. To decrease the complexity of the parameter space, all parameters were held constant except b_1 which has been shown to be important in the stability of predator–prey models (Murdoch & Oaten, 1975) and the exponent ϵ which was used to explore how the state space changed as the functional response varied. Therefore, equilibria were identified as functions of the parameters b_1 and ϵ, and the community matrix used to assess the stability of each equilibrium was derived. Several types of stability regions were outlined in the b_1–ϵ space to illustrate how the equilibrium qualitatively changes (e.g. from stable to unstable, or from limit cycles to chaos) as a function of b_1 and ϵ. The results of these analytical studies were used as a guide to direct the numerical simulations and to interpret those results. Analogously, for scenario 2, the stability was investigated by varying γ with ϵ set to one.

TABLE 1
Values of the non-dimensional parameters used for analytic and simulation study

Non-dimensional parameter	Values used
a_1	5.0
b_1	investigated between 2.0 and 12
a_2	0.1
b_2	2.0
d_1	0.4
d_2	0.01
Scenario 1:	
ϵ	investigated between 1.0 and 2.0
γ	0
Scenario 2:	
ϵ	1
γ	investigated between 0 and 2.0

The model was implemented on a Sun SPARC station using a custom program (written by Maszle) which uses an adaptive integration algorithm (Gear, 1969, 1971). Checks were implemented to assure that populations remained positive. Numerical simulations were run for 50000 time steps. The first portion of the sequence was thrown away, as it represented transient behavior, and only the last 20000 time steps were retained. The simulation time and the length of sequence to retain were determined empirically, since the time for the system to converge varied depending on the parameter values. This portion of the sequence was then considered to be on or near an attractor, which was either complex dynamics, a simple limit cycle, or a simple equilibrium. To facilitate convergence to steady-state behavior, the initial population values were set to 1% greater than the equilibrium found in the analytical analysis. The successive maxima of z were plotted against corresponding b_1 values at several values of either ϵ (Fig. 2) or γ (Fig. 3).

Figure 2 shows bifurcation diagrams of $z_{\max}$ as the parameter b_1 was varied. For any value of b_1, a small number of $z_{\max}$ values represent a limit cycle, the exact number determining the complexity of one cycle. Only one value at a given b_1 represents either a simple one-period cycle or a steady-state equilibrium. The doubling of the number of $z_{\max}$ as b_1 is increased is called period doubling. In Fig. 2(a), a sequence to period doublings occurs so rapidly that the number of $z_{\max}$ for a given b_1 becomes a black band. This is a strong indication of chaos (Eckmann & Ruelle, 1985).

Although the use of z-maxima plots is only suggestive of chaotic activity, we chose this method to enable a comparison between our results and those of Hastings and Powell. For the purposes of this study the

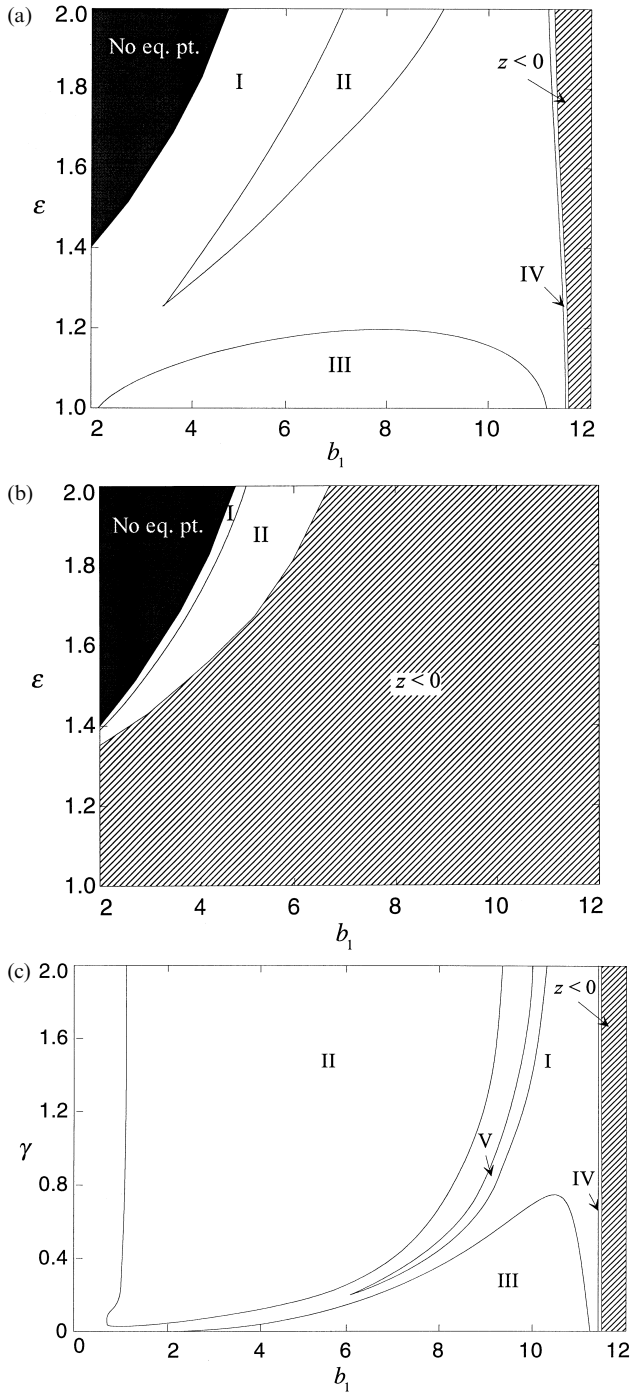

FIG. 1. (a) Stability regions for equilibrium $\bar{\mathbf{x}}_5^1$. No equilibria exist in the black region. The gray area contains no biologically possible equilibria as the population levels of z fall below 0. Region I: One stable and two oscillatory stable eigenvalues. Region II: Three stable eigenvalues. Region III: One stable and two oscillatory unstable eigenvalues. Region IV: Three stable eigenvalues. (b) Stability regions for equilibrium $\bar{\mathbf{x}}_6^1$. Shading is as in Fig. 1(a). Region I: One unstable, and two oscillatory unstable eigenvalues. Region II: One unstable and two oscillatory stable eigenvalues. (c) Stability regions for equilibrium $\bar{\mathbf{x}}_5^2$. Shading is as in Fig. 1(a) Region I: One stable and two oscillatory stable eigenvalues. Region II: One stable and two oscillatory unstable eigenvalues. Region III: One stable and two oscillatory unstable eigenvalues. Region IV: Three stable eigenvalues. Region V: Three stable eigenvalues.

evidence provided from the z-maxima plots of the existence of complex and potentially chaotic dynamics is sufficient.

Results

ANALYTICAL

To find the equilibrium points for the food chain model in eqn (1), each of the three equations were set equal to zero. For the types of functions we consider here, six equilibrium solutions exist, as discussed below and in the Appendix.

For both scenarios, four of the six equilibria [eqns (A.1–A.3), (A.4) and (A.7) in the Appendix] were considered trivial since they represent extinction of one or more species: $\bar{\mathbf{x}}_1$ represents global extinction; $\bar{\mathbf{x}}_2$ represents extinction of the two predator populations, with the autotroph remaining at its carrying capacity; $\bar{\mathbf{x}}_3$ represents coexistence of the autotroph with the first level predator; and $\bar{\mathbf{x}}_4$ represents coexistence of the two top level predators. In the absence of the autotroph, $\bar{\mathbf{x}}_4$ is unstable since y gains resources only from x, so the system in this state would lead to extinction of all species.

The fifth and sixth equilibria are expressed in a quadratic form and thus consist of a pair of positive and negative roots. These are the non-trivial steady state values where all three species coexist. Their stability conditions were determined by finding the community matrix and numerically calculating the eigenvalues over a range of b_1 and ϵ for scenario 1 and over a range of b_1 and γ for scenario 2.

For scenario 1, Figs 1(a) and 1(b) show how the stability characteristics of the equilibrium points $\bar{\mathbf{x}}_5^1$ and $\bar{\mathbf{x}}_6^1$ change with different values of b_1 and ϵ. Each region in these plots represents systems with similar characteristic behavior (see figure captions for the specific characteristics of each region). The borders surrounding the regions are lines of bifurcation where the system's behavior changes qualitatively with a slight change of a parameter value. The shaded regions indicate values of the parameters for which no equilibrium exists or for which there would be no equilibrium in a natural system (e.g. the equilibrium population would be negative). In region III of Fig. 1(a), the community matrix evaluated at $\bar{\mathbf{x}}_5^1$ has one stable eigenvalue with monotonic approach (negative real values) and two unstable oscillatory eigenvalues. Surrounding region III is an oscillatory but stable regime, region I; in the other two regions, II and IV, $\bar{\mathbf{x}}_5^1$ is a stable node (all three eigenvalues are negative and real).

Since all other biologically possible stability regions are stable ones, region III is the only candidate for

chaotic behavior. Thus, chaotic behavior is only possible for values of ϵ that are close to 1.0. The upper bound of region III of Fig. 1(a) was estimated to be about 1.17 by numerically calculating the eigenvalues at equilibrium $\bar{\mathbf{x}}_5^1$ at many points in the plane. For values of ϵ near 2.0, if the positive equilibrium point exists, it is either a stable node (region II) or an oscillatory stable node (region I). For intermediate ϵ values, the stable node disappears leaving only the stable, oscillatory behavior of region I.

For scenario 2, the z-value of $\bar{\mathbf{x}}_6^2$ is negative for the full range of b_1 and γ explored in this study and therefore would not exist in a natural system. Figure 1(c) shows the bifurcation diagram for the fifth equilibrium, $\bar{\mathbf{x}}_5^2$. Note that this parameter space is contiguous with that of Fig. 1(a) at the $\epsilon = 1.0$ and $\gamma = 0$ axes. There exist five regions of stability for equilibrium $\bar{\mathbf{x}}_5^2$: (i) region I is a snaking, irregular-shaped region winding between the other regions and having one stable eigenvalue with monotonic approach and two oscillatory stable eigenvalues; (ii) region II has one stable eigenvalue with monotonic approach and two oscillatory unstable eigenvalues; (iii) region III has the same stability characteristics as region II but is realized for low values of γ; (iv) region IV is a thin boundary region in which the equilibrium point has three stable eigenvalues with monotonic approach; and (v) region V is an island in the middle of region I with the same stability as region IV. Therefore, for this scenario, complex behavior is possible in a much larger space (regions II and III) than for scenario 1.

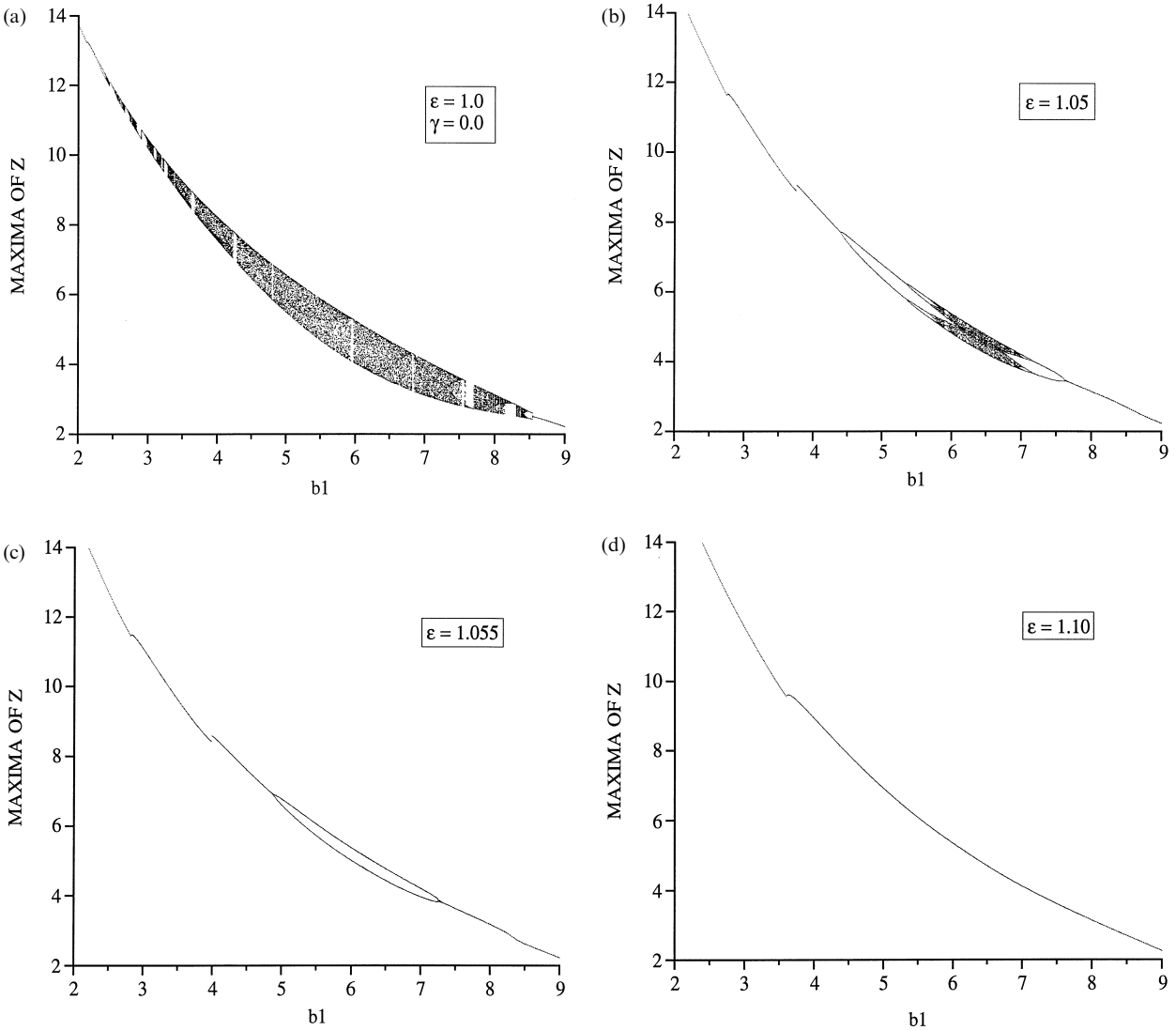

FIG. 2. Bifurcation diagrams of z_{max} as b_1 is varied, for increasing values of ϵ. (a) $\epsilon = 1$. (b) $\epsilon = 1.05$. (c) $\epsilon = 1.055$. (d) $\epsilon = 1.10$.

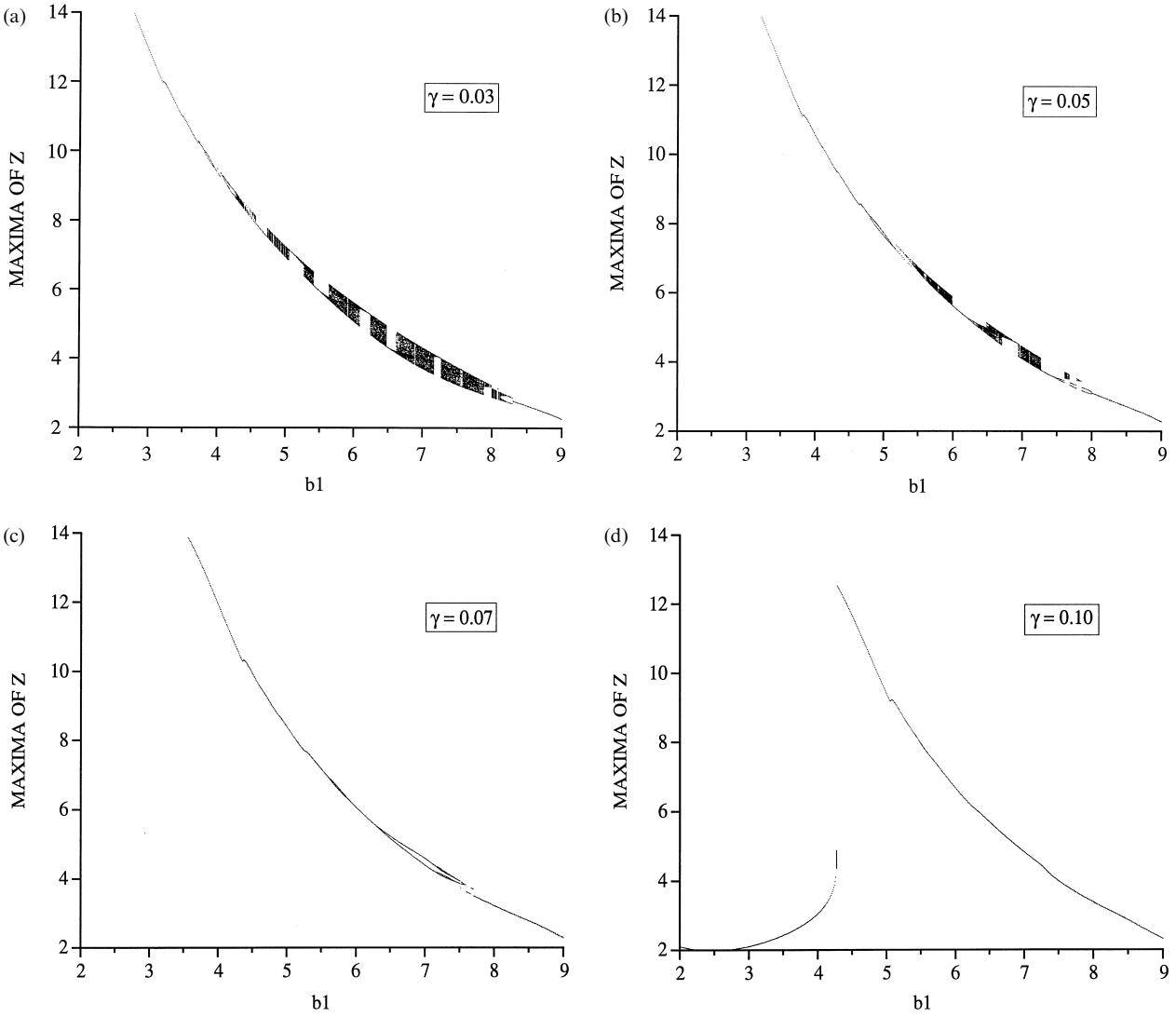

FIG. 3. Bifurcation diagrams of z_{max} as b_1 is varied, for increasing values of γ. (a) $\gamma = 0.03$. (b) $\gamma = 0.05$. (c) $\gamma = 0.07$. (d) $\gamma = 0.10$.

NUMERICAL

We numerically simulated the system of eqn (1) with the modified y–z interactions shown in eqn (5) in order to further investigate the sensitivity of system dynamics to varying either ϵ at values near 1 or γ at values near 0. For scenario 1, Figs 2(a)–(d) show a sequence of plots of z-maxima as a refuge effect was slowly added using four values of ϵ, 1.0, 1.05, 1.055 and 1.1. For scenario 2, Figs 3(a)–(d) show a sequence of plots of z-maxima as a territorial effect was slowly added by using increasing values of γ, 0.03, 0.05 and 0.07 and 0.1. Each bifurcation plot shows the results of many simulations, one at each ordinate value of the half-saturation constant, b_1. At each value of b_1 the global z-maxima were plotted.

In scenario 1, for small values of b_1 the system exhibited a stable node, and therefore the z-maxima were equal to the equilibrium value of z. As b_1 was incremented and the system began to show limit cycle behavior around the equilibrium, the z-maximum moved off the equilibrium value to the peak value of the limit cycle. For $\epsilon = 1.0$ and $\epsilon = 1.05$, incrementing b_1 further resulted in a split or bifurcation of a single z-maximum curve into two curves, then four, and so on. These splits are called period doublings and correspond to a doubling of the number of fundamental frequencies in the limit cycle (i.e. doubling the number of successive maxima that occur before the completion of one period). Each subsequent period doubling occurs over an increasingly smaller increment of b_1, so that an infinite number of period

doublings could occur with a finite change in the parameter value as shown by the dense portion of the graphs. An infinite sequence of period doublings is evidence, though not conclusive, that a system's behavior is chaotic.

In the bifurcation plots of Figs 2 and 3, a lower branch of local z-maxima bifurcations has been removed. This lower branch corresponds to the introduction of fast rise and fall fluctuations of the z predator population, even though the overall trend of the population is to increase to a global maximum density just before the population crashes. These fast dynamics were not indicative of a periodic doubling and so were removed in order to make the graphs more clear.

Figure 2(a) shows the bifurcation diagram of successive maxima of z as presented by Hastings and Powell (1991) for $\epsilon = 1.0$ and $\gamma = 0$. The period doubling sequence suggesting the existence of chaos is apparent. At $\epsilon = 1.05$, there also exists the possibility of chaotic behavior (Fig. 2b). The discontinuity near $b_1 = 2.75$ corresponds to where the system begins to show limit cycle behavior as the z maximum moves off its equilibrium value onto a limit cycle. This value of b_1 approximates the transition into region III from region I in Fig. 1(a). At about $b_1 = 4.4$, the first period doubling is seen, the second at 5.4, and the third and 5.7. For larger values of b_1 a period halving occurs as the system returns to less complicated limit cycle behavior. These plots suggest that as the refuge effect was added, the range of complex dynamics diminished with period doublings occuring for values of b_1 in the range 2.3–8.6 for $\epsilon = 1.0$, 4.4–7.7 for $\epsilon = 1.05$, 4.9–7.3 for $\epsilon = 1.055$. Further, for $\epsilon = 1.055$, only a single period doubling occurred, and no complex dynamics were found. For $\epsilon = 1.10$, the system exhibited either stable coexistence or a simple limit cycle. The narrowing of the range of complex dynamics and their eventual disappearance can be anticipated by recalling from Fig. 1(a) the shape of region III, the only place in which complex dynamics can occur. As ϵ is increased, the range of b_1 falling in this region narrows to zero.

As with ϵ in the first scenario, chaos was observed in scenario 2 for lower values of γ (Fig. 3). For $\gamma > 0.06$, the dynamics revert to simpler limit cycles, and progression to chaotic dynamics was not seen for the range of b_1 explored. As γ is slowly increased from 0 to 0.06, the onset of period doubling leading to potential chaotic dynamics begins at higher and higher values of b_1, and the range over which period doubling occur shrinks. At $\gamma = 0$, a period-doubling sequence begins at 2.3 and eventually unwinds through a period-halving sequence completing at approximately 8.6. For $b_1 > 8.6$, the system again exhibits a simple limit cycle. As γ is increased, the range of complex behavior shrinks to 3.8–8.3 for $\gamma = 0.03$, 4.8–8.0 for $\gamma = 0.05$, and 6.3–7.6 for $\gamma = 0.07$.

The range of complex behavior thus occurs for a narrower range of b_1, and the range is skewed to higher values of b_1. We can understand this shifting by noting in Fig. 1(c) the skewed shape of region III in which the complex dynamics are found. Unlike scenario 1, chaos is possible over a wide range of b_1 for all values of γ explored in this study (0 to 2) because of the stability characteristics of equilibrium $\bar{\mathbf{x}}_5^2$ in the b_1-γ parameter space [Fig. 1(c)], specifically those of region II. Numerically, such complex dynamics were not found for larger values of γ. For values of γ less than 4.28 Fig. 3(d) shows the emergence of a stable limit cycle existing between the equilibria $\bar{\mathbf{x}}_5^2$ and $\bar{\mathbf{x}}_6^2$. Though $\bar{\mathbf{x}}_6^2$ in this scenario does not correspond to a biological equilibrium, its stability characteristics affect the dynamics of the model.

Discussion

Thom (1972) first argued for the importance of structural stability in mathematical models of biological systems. More recently, structural stability analysis has been applied to ecological systems. In this context "structure" refers to the addition of a term or the change of a functional form beyond a simple parameter change, and is to be distinguished from the idea of food-web or community structure. DeAngelis (1989, 1992) discusses the common existence of structural instabilities in ecosystem models, citing examples in which food web structures are changed due to variations in environmental factors. Stone (1993) has shown that the existence of chaotic dynamics in a simple first-order nonlinear difference equation is sensitive to structural perturbations; our findings in this study are consistent with Stone's conclusion.

As the exponent ϵ was increased slightly above 1.0, we observed a rapid decrease in the complexity of the model dynamics. This outcome can be understood from Fig. 1(a). Region III marks the only portions of the b_1–ϵ parameter space in which the real parts of the eigenvalues are positive. Therefore this is the only location in which chaotic dynamics are possible. The condition under which the system remains in region III for the widest range of b_1 is $\epsilon = 1.0$, which corresponds to the one dimensional study of Hastings and Powell. Numerical simulations for $\epsilon = 1.0$ indicate that apparent chaos occurs within a range of b_1 between 2.4 and 8.6. However, Fig. 1(a) shows that as ϵ is increased, the range of b_1 inside region III decreases. This corresponds to Figs 2(a)–(c), where the narrowing of

the range in which chaos is observed is shown. As ϵ is increased further, chaotic dynamics are reduced to simple limit cycle behavior and then to stable equilibria as the system passes from the center of region III, to near the border, and then to region I [see Fig. 1(a)].

The shape of region III is skewed to the right [Fig. 1(a)] corresponding to the chaotic range shifting to the right with increasing ϵ. This is evident by looking at the "point of accumulation" where the rate of new period doublings becomes infinite and chaotic behavior ensues (i.e. the dense portion of the graphs). In Fig. 2(a) this occurs near $b_1 = 2.4$ for $\epsilon = 1.0$ and in Fig. 2(b) this occurs near $b_1 = 5.7$ for $\epsilon = 1.05$. Both graphs show a collapse of chaotic activity at approximately $b_1 = 6.5$ indicating that the range of b_1 for which chaos is possible as ϵ is increased from 1.0 to 1.05, is reduced and shifted.

Hassell & Comins (1978) showed that the use of a Holling Type III function resulted in a more stable prey-predator system than does the use of a Holling Type II. Our simulations support these conclusions. We found that for low values of b_1 the Holling III interaction does not allow coexistence of all three species, and for larger values of b_1, the Holling III interaction stabilizes the coexistent equilibrium $\bar{\mathbf{x}}_5^1$. That is, near the equilibrium point corresponding to coexistence, an increasing refuge effect ($\epsilon > 1.1$) eliminated chaos; for values of ϵ which lie in the wedge of region I, all oscillatory behavior ceased.

Our results further suggest that a slight refuge phenomenon or tapering off of predation at low densities would cause a collapse of the chaotic dynamics. The stability regions of Fig. 1(a) indicate that the stable dynamics seen for a Holling III interaction are insensitive to perturbations from $\epsilon = 2.0$, whereas the presence of chaos for a Holling II interaction is very sensitive to even slight changes in the exponent near $\epsilon = 1.0$, i.e., an increase in ϵ from 1.0 to 1.055 was sufficient to eliminate chaos. To assess the possibilities of chaotic dynamics in a species-specific three-trophic food chain model, sufficient data would be required to identify ϵ within a 5% uncertainty. It is unlikely that experimental data could distinguish between $\epsilon = 1.0$ and $\epsilon = 1.055$ when attempting to fit empirical functional response data to eqn (4). A comparison of plots of eqn (4) for $\epsilon = 1.0$, 1.055, and 2.0 is shown in Fig. 4. given the environmental variability seen in nature, it is unlikely that parameters such as ϵ are constant over time, thus compounding the problem of accurate parameter identification.

While chaotic behavior for this three-trophic model is not robust to a structural change of adding refugia in the absence of interference, the change in dynamics is not as predictable when perturbing the predator

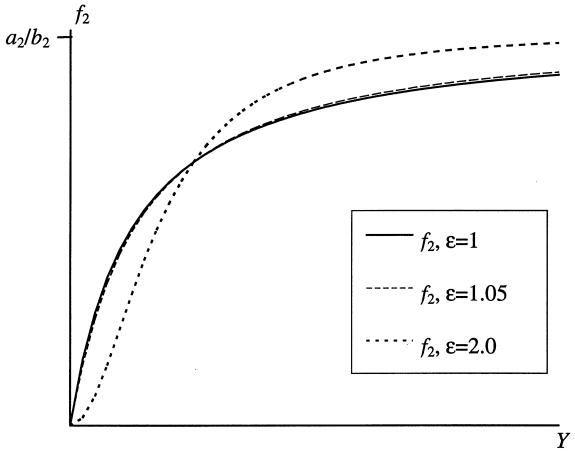

FIG. 4. Predator–prey interaction function for $\epsilon = 1.0$, 1.055 and 2.0.

interference parameter to non-zero values in the absence of refugia. For the particular parameter values chosen in this study, chaotic dynamics collapse into a stable equilibrium for values of $\gamma > 0.06$. As with the addition of refugia, chaotic dynamics are restricted to region III. Region III in the γ–b_1 parameter space is a narrowing right-skewed region as γ is increased, analogous to the ϵ–b_1 parameter space. Therefore, the numerical simulation plots of scenario 2 (Fig. 3) also show that the chaotic dynamics are found in a narrower and right-shifted region of b_1, suggesting that the system is still not robust in its chaotic mode.

However, while the addition of refugia is clearly a stabilizing influence, predator interference is not. In scenario 2, both regions II and III of Fig. 1(c) contain positive eigenvalues; therefore, region II cannot be precluded from the possibility of exhibiting complex dynamics. Even though the addition of predator interference was stabilizing using the parameter values from Table 1, this conclusion cannot be generalized to the whole parameter space.

Recently, the parameters used by Hastings and Powell were found to be biologically extreme (McCann & Yodzis, 1994). To obtain a biologically reasonable parameter set while maintaining the behavior seen by Hastings and Powell, McCann and Yodzis proposed to set $b_1 = 6.21$, $a_2 = 10d_2$, and to vary d_2 over the range 0.071–0.225. Our results for this new parameter set with respect to addition of refugia is similar to those using the original values. As ϵ is increased above 1.15, chaos is no longer possible. However, our overall conclusion that the structural sensitivity of a model is a critical aspect to analyzing dynamical behavior in ecosystems, is dependent on a specific parameterization. This is especially true in light of the concept of persistent chaos proposed by McCann & Yodzis

(1994). If a chaotic attractor is bounded close to a zero, any addition of small amounts of external noise will result in extinction of one or more of the species causing the system to collapse to simpler dynamics. Therefore, whether the chaotic attractor is close to the origin or it is contained in a relatively small volume, environmental fluctuations will cause the probability of observing complex dynamics to be small. Both of these features can be evaluated through sensitivity analyses.

To illustrate the importance of the information obtained through sensitivity analysis we chose to look at a narrow portion of the parameter space, concentrating on the sensitivity of identifying a predator consumption mechanism on the complexity of the dynamics. It would be impossible to extensively study all possible parameter combinations. Abrams & Roth (1994) expanded the scope of simulations by exploring a portion of the parameter space close to the one used by Hastings and Powell. In order to generalize our result that chaos is not very robust to varying conditions of refugia and consumer interference, a more thorough bifurcation analysis, as outlined by Klebanoff & Hastings (1994), would be necessary.

Though simple equations can easily exhibit chaos and ecosystems have all the ingredients of a chaotic system, it remains unclear how best to use these results to gain insight into the dynamics of natural ecosystems. Given that process descriptions are often phenomenological, understanding the structural stability of a model is an important step in gaining confidence in the applicability of a model inferring something about the real world. In addition to problems associated with the uncertainty of field data, parameter values most likely are not constant through time and dependent on many fluctuating environmental factors. As external conditions continually change, ecosystems are highly dynamic and rarely at steady state. These external conditions may cause perturbations to occur over various time scales (DeAngelis, 1992) such as gradually (e.g. geological and climatic changes); suddenly and permanently (e.g. change in stream flows); temporally in discrete events (e.g. fire, storms, or droughts); daily (e.g. wind or temperature); or natural periodicities (e.g. annual temperature and precipitation cycles). This dynamic disequilibrium description has been postulated to give rise to species diversity (Huston, 1979).

Therefore, through time, ecosystems may exhibit a variety of dynamics including chaos. A structural sensitivity analysis of this simple three-species model elucidated how the dynamics changed through the variation of two parameter values, suggesting in general that the existence of chaos is highly dependent on the structure of the model. Specifically, our analysis suggests that although this model could produce chaotic behavior, it is improbable given the smallness of the chaotic space and the sensitivity of the existence of such dynamics to small increases in ϵ or γ.

We would like to thank Jan Washburn and Wayne Getz for helpful comments on the manuscript. This research was funded by an NSF post-doctoral fellowship, grant #DEB-9303260 (awarded to J.E.) and an NIH training grant (awarded to D.M.). Order of authorship was determined by five flips of a coin and does not reflect priority with respect to contribution to the manuscript.

REFERENCES

Abrams, P. A. & Roth, J. D. (1994). The effects of enrichment of three-species food chains with nonlinear functional responses. *Ecology* **75,** 1118–1130.

Akcakaya, H. R. (1992). Population cycles of mammals—evidence for a ratio-dependent predation hypothesis. *Ecol. Monogr.* **62,** 119–142.

Arditi, R., Ginzgurg L. R. & Akcakaya, H. R. (1991*a*). Variation in plankton densities among lakes: a case for ratio-dependent predation models. *Am. Nat.* **138,** 1287–1296.

Arditi, R., Perrin, N. & Saiah, H. (1991*b*). Functional responses and heterogeneities: an experimental test with cladocerans. *Oikos* **60,** 69–75.

Arditi, R. & Saiah, H. (1992). Empirical evidence of the role of heterogeneity in ratio-dependent consumption. *Ecology* **73,** 1544–1551.

Berryman, A. A. (1992). The origins and evolution of predator-prey theory. *Ecology* **73,** 1530–1535.

DeAngelis, D. L. (1992). *Dynamics of Nutrient Cycling and Food Webs*, 1st edn. London: Chapman and Hall.

DeAngelis, D. L., Goldstein, R. A. & O'Neil, R. V. (1975). A model for trophic interaction. *Ecology* **56,** 881–892.

DeAngelis, D. L., Mulholland, P. J., Palumbo, A. V., Steinman, A. D., Huston, M. A. & Elwood, J. W. (1989). Nutrient dynamics and food-web stability. *A. Rev. Ecol. Syst.* **29,** 71–95.

Dixon, A. F. G. (1959). An experimental study of the searching behavior of the predator coccinellid beetle *Adalia decempunctata* (L). *J. Anim. Ecol.* **28,** 259–281.

Eckmann, J. P. & Ruelle, D. (1985). Ergodic theory of chaos and strange attractors. *Rev. Mod. Phys.* **57,** 617–656.

Gear, C. W. (1969). *The Automatic Integration of Stiff Ordinary Differential Equations*, pp. 187–193. Amsterdam: North Holland Publishing Company.

Gear, C. W. (1971). The automatic integration of ordinary differential equations. *Commun. ACM* **14,** 176–179.

Getz, W. M. (1984). Population dynamics: a per-capita resource approach. *J. theor. Biol.* **108,** 623–643.

Getz, W. M. (1993). Metaphysiological and evolutionary dynamics of populations exploiting constant and interactive resources—R-K selection revisited. *Evol. Ecol.* **7,** 287–305.

Gilpin, L. & Mackey, M. M. (1979). Spiral chaos in a predator-prey model. *Am. Nat.* **107,** 306–308.

Hassell, M. P. (1978). *The Dynamics of Arthropod Predator-Prey Systems*. Princeton, NJ: Princeton University Press.

Hassell, M. P. & Comins, H. N. (1978). Sigmoid functional responses and population stability. *Theor. Popul. Biol.* **14,** 62–67.

Hastings, A. & Higgins, K. (1994). Persistence of transients in spatially structured ecological models. *Science* **263,** 1133–1136.

Hastings, A. & Powell, T. (1991). Chaos in a three-species food chain. *Ecology* **72,** 896–903.

Holling, C. S. (1959). Some characteristics of simple types of predation and parasitism. *Can. Ent.* **91,** 385–398.

Huston, M. A. (1979). A general hypothesis on species diversity. *Am. Nat.* **113,** 81–101.

KLEBANOFF, A. & HASTINGS, A. (1994). Chaos in three species food chains. *J. math. Biol.* **32,** 427–451.
KREBS, J. R. (1974). *Behavioral Aspects of Predation*. New York: Plenum.
LOGAN, J. A. & HAIN, F. P. (1991). *Chaos and Ecology*. Blacksburg, VA: Virginia Agricultural Experiment Station, Virginia, Polytechnic Institute and State University.
MAY, R. M. & OSTER, G. F. (1976) Bifurcation and dynamic complexity in simple ecological models. *Am. Nat.* **110,** 573–599.
MCCANN, K. & YODZIS, P. (1994). Biological conditions for chaos in a three-species food chain. *Ecology* **75,** 561–564.
MURDOCH, W. W. (1969). Switching in general predators: experiments on predator specificity and stability of prey populations. *Ecol. Monogr.* **39,** 335–354.
MURDOCH, W. & OATEN, A. (1975). Predation and population stability. *Adv. Ecol. Res.* **9,** 1–125.
NUNNEY, L. (1980). The influence of the type 3 (sigmoid functional response upon the stability of predator-prey difference models. *Theor. Popul. Biol.* **18,** 257–278.
ORIANS, G. H. (1969). Age and hunting success in the brown pelican (*Pelecanus occidentalis*). *Anim. Beh.* **1,** 216–319.
REAL, L. A. (1977). The kinetics of functional response. *Am. Nat.* **111,** 289–300.
STONE, L. (1993). Period-doubling reversals and chaos in simple ecological models. *Nature* **365,** 617–620.
SUGIHARA, G. & MAY, R. M. (1990). Nonlinear forcasting as a way of distinguishing chaos from measurement error in time series. *Nature* **344,** 734–741.
THOM, R. (1972). Structural stability and morphogenesis: an outline of a general theory of models. New York: Addison–Wesley.
WOLFRAM, S. (1991). *Mathematica*: *a System for Doing Mathematics by Computer*. Redwood City, CA: Addison–Wesley.

APPENDIX

Listed below are the six equilibrium points for both scenarios that were shown to exist using the software package *Mathematica*® (Wolfram, 1991).

Equilibrium points $\bar{\mathbf{x}}_1$, $\bar{\mathbf{x}}_2$, and $\bar{\mathbf{x}}_3$ for both scenarios 1 and 2.

$$\bar{\mathbf{x}}_1^1, \bar{\mathbf{x}}_1^2: \quad \{\bar{x}, \bar{y}, \bar{z}\} = \{0, 0, 0\} \tag{A.1}$$

$$\bar{\mathbf{x}}_2^1, \bar{\mathbf{x}}_2^2: \quad \{\bar{x}, \bar{y}, \bar{z}\} = \{1, 0, 0\} \tag{A.2}$$

$$\bar{\mathbf{x}}_3^1, \bar{\mathbf{x}}_3^2: \quad \{\bar{x}, \bar{y}, \bar{z}\} = \left\{\frac{d_1}{a_1 - b_1 d_1}, \frac{a_1 - d_1 - b_1 d_1}{(a_1 - b_1 d_1)^2}, 0\right\}. \tag{A.3}$$

Equilibrium points $\bar{\mathbf{x}}_4$, $\bar{\mathbf{x}}_5$, and $\bar{\mathbf{x}}_6$ for scenario 1.

$$\bar{\mathbf{x}}_4^1: \quad \{\bar{x}, \bar{y}, \bar{z}\} = \left\{0, \sqrt[\epsilon]{\frac{d_2}{a_2 - b_2 d_2}}, \frac{d_1}{d_2}\bar{y}\right\} \tag{A.4}$$

$$\bar{\mathbf{x}}_5^1: \quad \{\bar{x}, \bar{y}, \bar{z}\} = \{R_1 + \tfrac{1}{2}\sqrt{R_2}, \sqrt[\epsilon]{R_3}, R_4\} \tag{A.5}$$

$$\bar{\mathbf{x}}_6^1: \quad \{\bar{x}, \bar{y}, \bar{z}\} = \{R_1 - \tfrac{1}{2}\sqrt{R_2}, \sqrt[\epsilon]{R_3}, R_4\}, \tag{A.6}$$

where

$$R_1 = \frac{b_1 - 1}{2b_1}, \; R_2 = (2 \cdot R_1)^2 - 4\frac{a_1\bar{y} - 1}{b_1}, \; R_3 = \frac{d_2}{a_2 - b_2 d_2}$$

$$R_4 = \frac{\bar{y}}{a_2 \bar{y}^{\epsilon}}\left(\frac{a_1 \bar{x}}{1 + b_1 \bar{x}} - d_1\right)(1 + b_2 \bar{y}^{\epsilon}).$$

Equilibrium points $\bar{\mathbf{x}}_4$, $\bar{\mathbf{x}}_5$, and $\bar{\mathbf{x}}_6$ for scenario 2.

$$\bar{\mathbf{x}}_4^2: \quad \{\bar{x}, \bar{y}, \bar{z}\} = \left\{0, \frac{-a_2}{-(b_2 + g) \cdot d_1}, \frac{-d_1}{(b_2 + g) \cdot d_1}\right\} \tag{A.7}$$

$$\bar{\mathbf{x}}_5^2: \quad \{\bar{x}, \bar{y}, \bar{z}\} = \{R_5 + \tfrac{1}{2}\sqrt{R_6}, R_7, R_8\} \tag{A.8}$$

$$\bar{\mathbf{x}}_6^2: \quad \{\bar{x}, \bar{y}, \bar{z}\} = \{R_5 - \tfrac{1}{2}\sqrt{R_6}, R_7, R_8\}, \tag{A.9}$$

where R_5–R_8 are complex expressions of the parameters.